A spectral model for turbulence and microphysics dynamics in an ice cloud

A. J. Palmer

Nonlinear Processes in Geophysics (1996) 3: 23 - 28

Nonlinear Processes in Geophysics

A spectral model for turbulence and microphysics dynamics in an ice cloud

A. J. Palmer

NOAA, Environmental Technology Laboratory, 325 Broadway, Boulder, CO 80303, USA

Received 30 June 1995 - Accepted 27 January 1996 - Communicated by L. A. Ostrovsky

Abstract. A one-dimensional, nine-mode spectral model for temperature, velocity, and the mixing ratios of suspended and precipitating ice-particle components is shown to be consistent with ice-cloud observations. The observations include Doppler radar time-series measurements of a single winter ice cloud and direct measurements of mean particle size vs. ice-water content for a set of ice clouds. Fitting of the model to the Doppler vertical-velocity measurements allows a prediction to be made of the vertical scale and turbulent Prandtl number active in the ice-cloud vertical motions. The model is then used to explore the question of how turbulence and gravity-wave motions affect the microphysical properties of an ice cloud. The model predicts interesting dynamical effects on the mixing ratios due to these motions, but no significant effects on the time-averaged microphysical quantities.

1 Introduction

Ice clouds are synoptic and mesoscale systems that make important contributions to the radiative balance of the earth's atmosphere. They are currently under intensive study because of the need to better understand their role in the potential climate change induced by anthropogenic injections of radiatively active gases into the atmosphere. Of particular interest is the feedback response of ice clouds to global warming. Because ice clouds are not blackbody radiators, their radiative properties and feedback response will depend on the size, shape, and concentration of the ice particles and the dependence of these microphysical properties on cloud ambient conditions.

Ice clouds are also interesting, open, nonlinear dynamical systems on time scales associated with stable-layer gravity-wave and turbulent motions. These dynamical motions are not resolved by climate models and have not been explicitly included in recent microphysical models of ice clouds. These motions are important to understand in their own right, and a particularly relevant question for the climate impact of ice clouds is whether or not these motions significantly influence the radiatively important microphysical properties of the cloud.

In this paper, we utilize a simple truncated spectral model of stable-layer turbulence coupled to a two-component Kessler-type model (Kessler, 1969; Wacker, 1992) of the ice-particle growth and removal processes in order to address both of these issues. Comparison of the model with ice-cloud measurements found in Palmer and Martner (1995) suggests that the model captures some of the dynamics of ice-cloud microphysics. The model results also suggest that the common practice of modeling the time-averaged microphysical properties of an ice cloud separately from the turbulent dynamics is probably an acceptable approximation.

2 Thermodynamics

The thermodynamics portion of the model is a simple truncated spectral model known as the Burgers-Chao model (Zheng and Liu, 1993). In this model both the velocity and temperature fields in the one-dimensional Navier Stokes equations are separated into a vertically averaged component dependent only on time and a perturbed component dependent on time and the vertical coordinate. An attractive feature of this model is that aperiodic behavior is found for flow parameters that are reasonable for turbulence in atmospheric stable layers such as are found in ice clouds. In Zheng and Liu (1993), the nonlinear dynamical properties of these equations were examined for stable stratification conditions and for a Prandtl number equal to unity. Fixed-point, limit-cycle, and chaotic dynamical attractors were found to be generated by these equations for values of the Reynolds number and Richardson number that occur in the atmospheric boundary layer. Recently, in an attempt to model the turbulence dynamics in a weak stable layer within a marine stratus cloud, these equations were expanded to include an arbitrary

Prandtl number and liquid-water dynamical variables, with the latter's contribution to latent heat transfer and buoyancy (Palmer, 1995). We use an analogous set of equations for the temperature and velocity fields here:

$$dU(t)/dt = P - \nu \Pr U(t)/H^2 - 1/H^2 \int_0^H w(z,t)^2\, dz \qquad (1)$$

$$\partial w(z,t)/\partial t = U(t)\, w(z,t)/H + \Pr \nu \partial^2 w(z,t)/\partial z^2 - w(z,t)\, \partial w(z,t)/\partial z + g\left[\theta_L(z,t) + L\rho q_s/c_p\right]/\langle\Theta_L\rangle \qquad (2)$$

$$d\Theta_L(t)/dt = Q - \nu\Theta_L(t)/H^2 - 1/H^2 \int_0^H w(z,t)\,\theta(z,t)\, dz \qquad (3)$$

$$\partial\theta_L(z,t)/\partial t = \left[\Theta_L(t)/H - \gamma_a\right] w(z,t) + \nu\partial^2\theta_L(z,t)/\partial z^2 - w(z,t)\,\partial\theta_L(z,t)/\partial z\,, \qquad (4)$$

where t is time; z is the vertical coordinate; $U(t)$ and $\Theta_L(t)$ are the vertically averaged horizontal velocity and ice-water potential temperature (Deardorff, 1976), respectively; and $w(z,t)$ and $\theta_L(z,t)$ are the perturbed values of the vertical velocity and ice-water potential temperature, respectively. P is the pressure gradient force and Q is the heat source, both of which are necessary to maintain the initial values of $U(t)$ and $\Theta_L(t)$. Pr is the turbulent Prandtl number (henceforth, Prandtl number will mean turbulent Prandtl number), ν is the eddy heat conductivity, H is the vertical scale of the model, γ_a is the moist adiabatic lapse rate, L is the ice latent heat of evaporation, c_p is the atmosphere's specific heat, and g is the acceleration of gravity. In the buoyancy term, we have assumed saturation conditions and have approximated the background and perturbed virtual potential temperatures as (Palmer, 1995)

$$\langle\Theta_v\rangle \sim \langle\Theta_L\rangle \qquad (5)$$

$$\theta_v \sim \theta_L + L\rho q_s/c_p\,, \qquad (6)$$

where q_s is the perturbed component of the suspended ice-particle mixing ratio defined further below, ρ is the ambient atmospheric density, and $\langle\rangle$ indicates the temporal average.

3 Microphysics

We choose a simple two-component Kessler-type model to describe the ice-cloud microphysical processes. The two components are a precipitating component and a suspended component. A zero-dimensional model of this type applied to water and mixed-phase clouds in the absence of advection was examined by Wacker (1992). The model was shown to give rise to both fixed-point and limit-cycle dynamical behavior for a mixed-phase cloud (Wacker, 1992). Chaotic dynamics corresponding to the turbulence behavior observed in radar measurements of clouds cannot be reproduced by this two-component model since a minimum of three nonlinearly coupled degrees of freedom are required for a dynamical system to exhibit chaos.

In order to treat the turbulent microphysics dynamics observed in the ice-cloud radar reflectivities, we simply enlarge the zero-dimensional model used in Wacker (1992) to a one-dimensional model using the same Burger-type approximation as used above for the velocity and temperature fields. With the assumption that only the suspended component participates in the vertical transport, the dynamical equations for the ice-particle mixing ratios become

$$dQ_s(t)/dt = \phi_s - bQ_s(t)\, Q_p(t)^\beta - \mathrm{Pri}\, Q_s(t)/H^2 - 1/H^2 \int_0^H w(z,t)\, q_s(z,t)\, dz \qquad (7)$$

$$\partial q_s(z,t)/\partial t = -bq_s(z,t)\, Q_p(t)^\beta + Q_s(t)\, w(z,t)/H + \mathrm{Pri}\,\nu\,\partial^2 q_s(z,t)/\partial z^2 - w(z,t)\,\partial q_s(z,t)/\partial z \qquad (8)$$

$$dQ_p(t)/dt = \phi_p + b\, Q_s(t)\, Q_p(t)^\beta - dQ_p(t)\,, \qquad (9)$$

where $Q_s(t)$ and $q_s(z,t)$ are the vertically averaged and perturbed suspended component mixing ratios; $Q_p(t)$ is the vertically averaged precipitating component mixing ratio; ϕ_s and ϕ_p are the source rates for the suspended and precipitating components, respectively; Pri is the turbulent Prandtl number for ice-particle diffusion (ratio of suspended component particle diffusion coefficient to thermal diffusion coefficient); b is the coefficient of accretion; β is the exponent of accretion; and d is the coefficient of sedimentation flux for the precipitating particles (Wacker, 1992).

The above set of partial differential equations was converted to ordinary differential equations, using the usual spectral truncation with Dirichlet boundary conditions:

$$w(z,t) = w_1(t)\sin(\pi z/H) \qquad (10)$$

$$\theta_L(z,t) = \theta_1(t)\sin(\pi z/H) - \theta_2(t)\sin(2\pi z/H) \qquad (11)$$

$$q_s(z,t) = q_{s1}(t)\sin(\pi z/H) - q_{s2}(t)\sin(2\pi z/H)\,. \qquad (12)$$

After converting to dimensionless variables, these substitutions result in the following set of ordinary differential equations for nine spectral modes:

$$\dot{x}_1 = \Pr(1 - x_1 - 1/2\, x_2^2) \qquad (13)$$

$$\dot{x}_2 = \Pr\left[(\mathrm{Re}\, x_1 - \pi^2)\, x_2 + x_4\right] + b1\, q_{s1} \qquad (14)$$

$$\dot{x}_3 = 1 - x_3 - (a/2)\, x_2\, x_4 \qquad (15)$$

$$\dot{x}_4 = c\,(x_3 - \gamma_a/\gamma_0)\, x_2 - \pi^2 x_4 - \pi\, x_2 x_5 \qquad (16)$$

$$\dot{x}_5 = -4\pi^2 x_5 + (\pi/2)\,\mathrm{Re}\,\Pr^2\, x_2 x_4 \qquad (17)$$

$$\dot{Q}_s = \phi_s' - b' Q_s Q_p^{\beta} - \mathrm{Pri}\, Q_s - 1/2\ \mathrm{Pr}\ \mathrm{Re}^{1/2} x_2 q_{s1} \quad (18)$$

$$\dot{q}_{s1} = \mathrm{Pr}\ \mathrm{Re}^{1/2} Q_s x_2 - b' q_{s1} Q_p^{\beta} - \mathrm{Pri}\, \pi^2 q_{s1} - \mathrm{Re}^{1/2}\ \mathrm{Pr}\ \pi\, q_{s2}\, x_2 \quad (19)$$

$$\dot{q}_{s2} = -b' q_{s2} Q_p^{\beta} - 4\pi^2\ \mathrm{Pri}\ q_{s2} + \mathrm{Re}^{1/2}\ \mathrm{Pr}\ \pi\, x_2 q_{s1} \quad (20)$$

$$\dot{Q}_p = \phi_p' + b' Q_s Q_p^{\beta} - d' Q_p, \quad (21)$$

where the dimensionless velocity and temperature variables are defined as

$$x_1 = U/U_0;\ U_0 = P H/(\mathrm{Pr}\ \nu) \quad (22)$$

$$x_2 = w_1/\sqrt{P} \quad (23)$$

$$x_3 = \Theta_L/\Theta_{L0};\ \Theta_{L0} = Q H/\nu \quad (24)$$

$$x_4 = \theta_1 \Big/ \left[\nu\ \mathrm{Pr}\ \sqrt{P}/(H^2\beta)\right] \quad (25)$$

$$x_5 = \theta_2 \Big/ \left[\mathrm{Pr}\ \nu^2/(H^3\beta)\right]. \quad (26)$$

The over-dot indicates a derivative with respect to the dimensionless time given by

$$\tau = (\nu/H^2)\, t \quad (27)$$

and

$$a = \mathrm{Pr}\,(\gamma_a/\gamma_0 - 1)/(\mathrm{Ri}\ \mathrm{Re}) \quad (28)$$

$$b1 = \mathrm{Re}^{3/2}\ \mathrm{Ri}\left[L\rho/(c_p \Theta_{L0})\right]/(\gamma_a/\gamma_0 - 1) \quad (29)$$

$$c = \mathrm{Pr}\ \mathrm{Ri}\ \mathrm{Re}^2/(\gamma_a/\gamma_0 - 1) \quad (30)$$

$$\gamma_0 = \Theta_{L0}/H \quad (31)$$

$$\beta = g/\Theta_L \quad (32)$$

$$(\phi_s', \phi_p', b', d') = (H^2/\nu)\,(\phi_s, \phi_p, b, d), \quad (33)$$

where Re and Ri are the Reynolds number and Richardson number for the model, respectively.

4 Model Comparison with Measurements

The first set of ice-cloud measurements that we use to compare the model to is the set of radar vertical-velocity measurements reported in Palmer and Martner (1995). In that work, the turbulent motions of a winter ice cloud in Colorado were measured with a 35-GHz Doppler radar. Vertical winds were obtained in the cloud using a vertically pointing, fixed-beam operating mode for the radar. The winds were sampled at midlevel in the cloud once every 3 s during a 9.6-h period. This time series showed clear evidence of both turbulent motions and a longer time-scale gravity wave with a period of 10 min. The turbulent motions were further characterized in that work by computing the correlation dimension for the time series, using a time-delay embedding method (Grassburger and Procaccia, 1983). When correctly applied, computation of the correlation dimension has been shown to be effective in delineating the dynamics underlying the data (Tsonis et al., 1994).

The parameters used for the model runs described below are listed in Table 1. The first thing to notice in comparing the model with the vertical motions observed by Palmer and Martner (1995) is that the model will also produce both gravity-wave motion and turbulent motion (Palmer, 1995; Zheng and Liu, 1993). However, it is clear from the measurements that the observed gravity-wave and turbulent motions occur on different vertical scales, and the model has only a single vertical scale. If the scale heights are disparate enough, it is reasonable to simply add together two model-generated time series for the two scale heights, and this was our procedure in comparing the modeled and observed vertical velocities. For the lapse rate and horizontal winds measured in the ice cloud, the model was found to best reproduce the observed gravity-wave period and velocity amplitude for a scale height and Prandtl number chosen near the values $H \sim 1$ km and $\mathrm{Pr} \sim 4$. To best reproduce the observed properties of the turbulent component of the vertical velocity, including the value for the correlation dimension, a scale height and Prandtl number of $H \sim 30$ m and $\mathrm{Pr} \sim 10$ were needed.

Table 1. Parameter values used in model.

Parameter	Values Used
U_0	20 m s^{-1}
γ_0; γ_a	0.008°C m-1; 0.01°C m^{-1}
Θ_0	-30°C
H	30 m, 1 km
Pr	10 (H = 30 m), 4 (H = 1 km)
Pri	Pr
ν	10 m^2 s^{-1} (H = 30 m), 100 m^2 s^{-1} (H = 1 km)
Ri	0.35 (H = 30 m), 0.5 (H = 1 km)
b	1081 s^{-1} (Wacker, 1992)
β	1.4 (Wacker, 1992)
d	1 × 10^{-2} s^{-1} (Wacker, 1992)
ϕ_p	1 × 10^{-8} s^{-1}
ϕ_{np}	1 × 10^{-8} – 1 × 10^{-5} s^{-1}
s_1; s_2	0.3 mm; 1.5 mm
C	5 mm^3 m^3 g

The autocovariance of the superposed modeled gravity-wave and turbulent vertical-velocity time series is shown in Fig. 1. This autocovariance looks qualitatively similar to the autocovariance reported in Palmer and Martner (1995), which is shown in the inset of Fig. 1. The principal differences can be accounted for by nonstationary trends in the data, which we do not attempt to model. The correlation dimension was also computed for the modeled velocity time series using the same time-delay embedding method as was used for the radar measurements (Grassburger and Procaccia, 1983). Among the criteria required for the correlation to be a reasonable estimate of the dynamical attractor dimension is that a large number of uncorrelated samples be used. In our computation of the correlation dimension, we used 1000 points at a sampling interval of 30 s for which the autocorrelation had dropped below $1/e$. The correlation dimensions for the model and for the measurements are compared in Table 2.

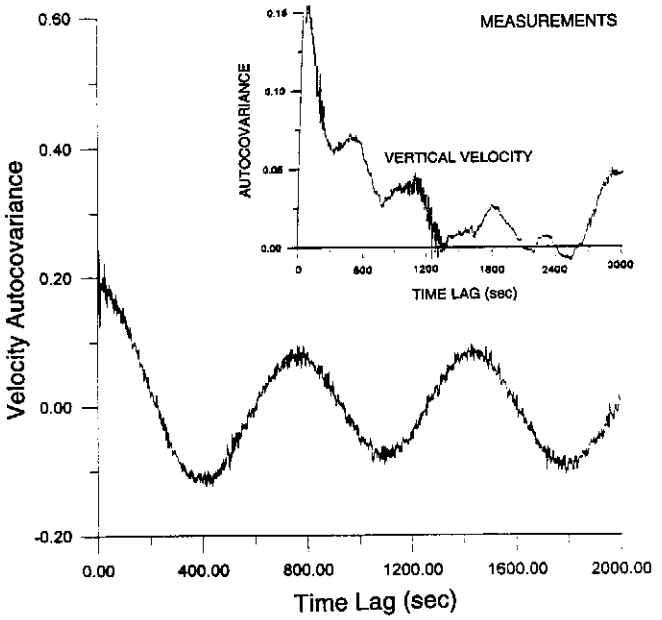

Fig. 1. Autocovariance of model-generated vertical velocity for a 1-km-scale gravity-wave time series added to a model-generated 30-m-scale turbulence time series. Inset shows the measured velocity autocovariance for an ice cloud reported in Palmer and Martner (1995).

The autocovariance and correlation dimension of the radar reflectivity time series for the ice cloud was also reported in Palmer and Martner (1995). Within the context of the two-component ice-particle model described above, the radar reflectivity can be assumed to be proportional to a weighted sum of the concentration of the two components, with the largest weighting applied to the precipitating component. The weighting factors were chosen to be proportional to the sixth power of the size distribution weighting factors, s_1 and s_2, used below in order to correspond with the dependence of the radar-scattering cross section on the sixth power of the particle diameter in the Rayleigh scattering regime.

Table 2. Correlation dimensions for measured and modeled time series.

	Measurements	Model
Vertical velocity	3.2	3.8
Radar reflectivity	2.3	2.9

A time series for the modeled radar reflectivity was generated by running the model under the same conditions used to generate the turbulent vertical-velocity time series discussed above. Unlike the measured velocity autocovariance, the reflectivity autocovariance reported in Palmer and Martner (1995) is not useful for model comparisons because it is dominated by nonstationary time behavior, which is beyond the scope of the model. However, the correlation dimension computed for the measured-reflectivity time series can be used for model comparison. The correlation dimensions computed for the measured- and modeled-reflectivity time series are compared in Table 2. The lower correlation dimension for both the measured- and modeled-reflectivity time series compared with that for the velocity time series is explainable as a result of the relatively weak coupling of the ice-particle concentrations with the velocity dynamics (Palmer, 1995). This is an example of the explanation put forward by Lorenz (1991) for the occurrence of low-dimensional attractors found in some weather and climate time series, wherein a fixed precision evaluation of the correlation dimension will be lower for the more weakly coupled variables. The fact that the correlation dimensions for the measured time series are lower than those for the corresponding modeled time series can probably be accounted for by nonstationary trends in the measured data.

The final ice-cloud observational dataset that we use to compare to the model is a plot of ice-cloud mean particle size vs. ice-water content reported in Heymsfield (1977) for many different ice-cloud systems. This particle size distribution is an important property of ice clouds in relation to their radiative effects on climate. In particular, Stephens et al. (1990) have shown that the particle size distribution in ice clouds is important in determining not only their contribution to the radiative balance of the atmosphere, but also their feedback response to an increase of CO_2 concentration in the atmosphere.

To compute the mean particle size and ice-water content from the above model, we define these quantities as time-averaged weighted sums of the two particle components:

$$\text{size} = \left\langle s_1 (Q_s + q_s) + s_2 Q_p \right\rangle \Big/ \left\langle Q_s + q_s + Q_p \right\rangle \tag{34}$$

$$\text{iwc} = \left\langle s_1^3 (Q_s + q_s) + s_2^3 Q_p \right\rangle \Big/ C, \tag{35}$$

where s_1 and s_2 are the weighting factors, and C is a normalization factor. To generate a particle size distribution, several time series were generated for a range of values for the small particle source rate, ϕ_s. The weighting factors, chosen to achieve a best fit with the observation data, are listed in Table 1. Figure 2 compares the computed mean particle size as a function of mean ice-water concentration with representative measurements taken from Heymsfield (1977). The agreement with the measurements is reasonable considering the restriction of the model to just two size components.

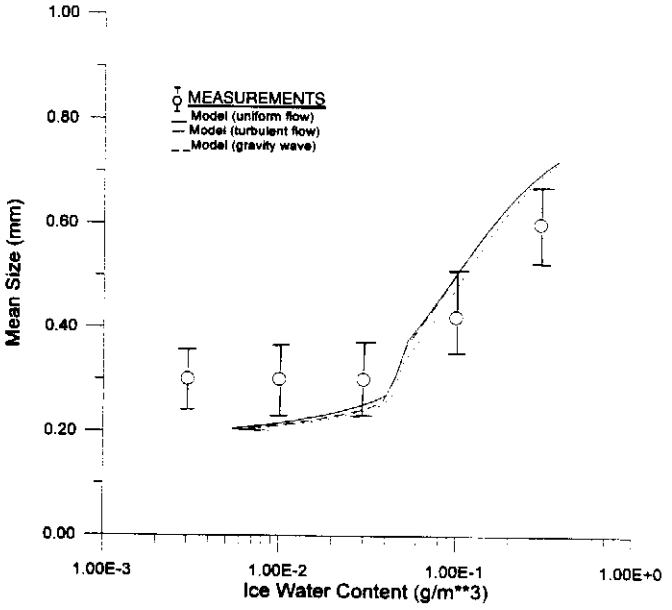

Fig. 2. Modeled mean particle size vs. ice-water content for various flow regimes compared to representative measurements from Heymsfield (1977).

5 Model Predictions

If the validations presented above are accepted as evidence that the model captures some of the basic dynamical behavior of ice-cloud microphysics, then questions regarding the dynamical interactions between the vertical motions and accretion processes in the cloud can be addressed by the model. As an example, we may ask whether, within the context of this simple model, changes in the vertical motion regimes, e.g., turbulent (chaotic), gravity-wave (limit cycle), or laminar flow (fixed point), will cause significant changes in either the dynamical or time-averaged microphysical properties of the ice cloud.

An example of an interesting dynamical interaction of this type was found by examining the time behavior of the two mixing ratios in a limit-cycle regime inherent in the zero-dimensional model already discovered in Wacker (1992). In this regime, a sensitivity to near-synchronous periodic forcing by gravity-wave-induced transport might be expected. An example of this behavior is presented in Fig. 3, which shows Poincare sections of the dynamical attractor with the two mixing ratios as coordinates. We see that the gravity-wave transport of the suspended component has forced the limit-cycle dynamics onto a chaotic attractor. This phenomenon is analogous to the known transition to chaos that can occur in periodic forced nonlinear oscillators (Tomita and Kai, 1978).

While the model shows that significant flow-induced changes in the time behavior of the microphysical variables can occur, such as in the above example, their time-averaged properties were found not to be significantly altered by the various flow regimes. As shown in Fig. 2, neither turbulent nor gravity-

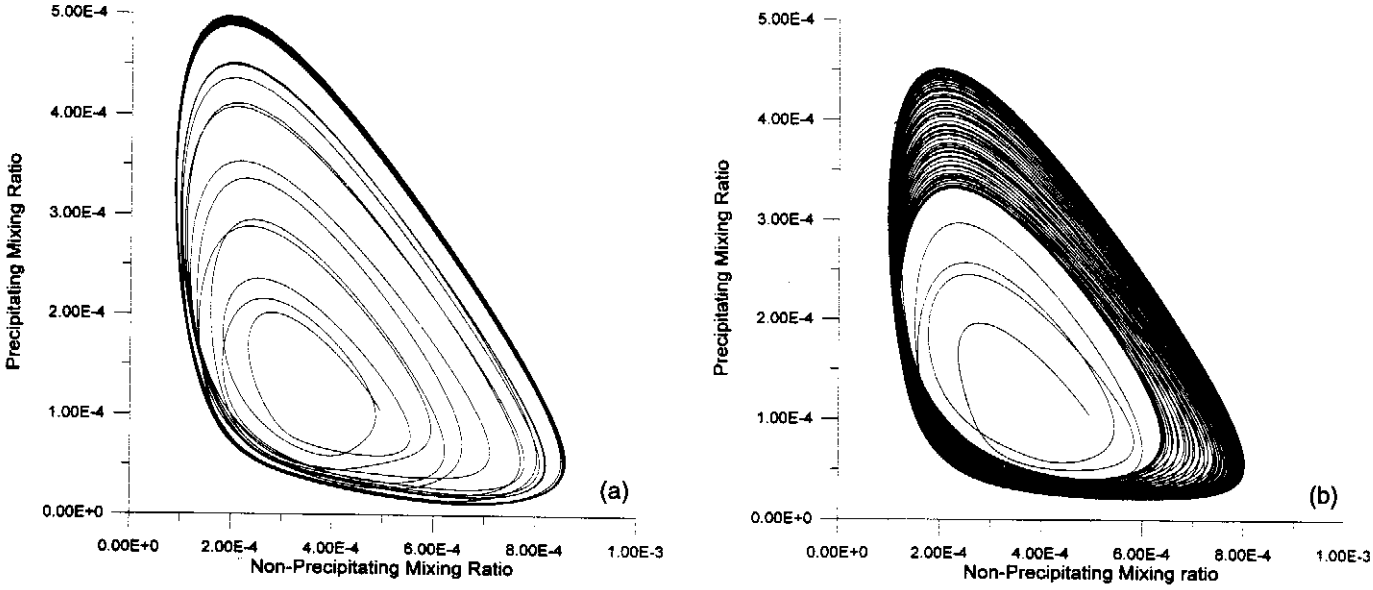

Fig. 3. Modeled dynamical attractor Poincare section for ice-particle mixing ratios showing (a) limit-cycle behavior for laminar flow, and (b) chaotic behavior for gravity-wave flow.

wave motions cause significant changes in the modeled mean particle size distribution curves. In generating the curves in Fig. 2, care was taken to average only over the structurally stable dynamical attractor, omitting transients. Also, several vertical scales for the model were examined. The vertical scale determines the ice-water content regime where the time scales for the flow dynamics and particle concentration dynamics are similar, and where one might expect evidence of coupling to the flow dynamics to appear. However, no significant dependence on this parameter was evident. The sharp upturn of the curve can be traced to the Hopf bifurcation in the solution to the mixing ratio equations already noted in Wacker (1992), and the presence of both turbulence and gravity-wave motion is seen to just smooth this transition slightly.

6 Conclusions

A simple truncated spectral model for temperature and velocity fields coupled to a two-component model for the ice-particle mixing ratios has been shown to be consistent with ice-cloud observations. The observations included Doppler radar time-series measurements of an ice cloud and mean particle size measurements as a function of ice-water content for a large set of ice clouds. Fitting of the model to the Doppler vertical-velocity measurements allowed a prediction to be made of the vertical scale and turbulent Prandtl number active in the ice-cloud vertical motions. The model was also used to explore the question of how turbulence and gravity-wave motions affect the microphysical properties of an ice cloud. The model predicts interesting dynamical effects on the mixing ratios, but no significant effects on the parametric behavior of time-averaged quantities. Further applications of the model might include development of ice-cloud parameterizations useful in climate models.

References

Deardorff, J.W., Usefulness of liquid-water potential temperature in a shallow-cloud model, *J. Appl. Meteor.*, *15*, 98–102, 1976.

Grassburger, P. and Procaccia, I., Characteristics of strange attractors, *Phys. Rev. Lett.*, *50*, 346–349, 1983.

Heymsfield, A.J., Precipitation development in stratiform ice clouds: A microphysical and dynamical study, *J. Atmos. Sci.*, *34*, 367–381, 1977.

Kessler, E., On the distribution and continuity of water substance in atmospheric circulations, *Meteor. Monogr.*, *10*, 84–103, 1969.

Lorenz, E.N., Dimension of weather and climate attractors, *Nature*, *353*, 241–244, 1991.

Palmer, A.J., Nonlinear dynamical analysis of turbulence in a stable cloud layer, *Chaos*, *5*, 311–316, 1995.

Palmer, A.J. and Martner, B.E., Radar measurements of turbulent dynamics in an ice cloud, *Proceedings, 27th Conf. on Radar Meteorology*, 9–13 October 1995, Vail, Colorado, pp. 586–588, 1995.

Stephens, G.L., Tsay, B.E., Stackhouse, P.W., Jr., and Flatau, P.J., The relevance of the microphysical and radiative properties of cirrus clouds to climate and climate feedback, *J. Atmos. Sci.*, *47*, 1742–1752, 1990.

Tomita, K. and Kai, T., Stroboscopic phase portrait and strange attractors, *Phys. Lett.*, *66A*, 91–93, 1978.

Tsonis, A.A., Triantafyllou, G.N., Elsner, J.B., Holdzkom, J.J., II, and Kirwan, A.D., Jr., An investigation of the ability of nonlinear methods to infer dynamics from observables, *Bull. Amer. Meteor. Soc.*, *75*, 1623–1633, 1994.

Wacker, U., Structural stability in cloud physics using parameterized microphysics, *Beitr. Phys. Atmos.*, *65*, 231–242, 1992.

Zheng, Z. and Liu, S., A nonlinear dynamical model for atmospheric boundary layer turbulence, *Chaos*, *3*, 305–312, 1993.